

H_∞ control of Industrial Emulator with backlash

M2014SC003 Masatsugu HIBINO

Supervisor : Isao TAKAMI

Abstract

The objective of this study is improving the performance of positioning control by using H_∞ control theory. In general, a backlash which has nonlinear characteristic exists between a gear and gears or gear and belts. Therefore, considering backlash is necessary to realize accurate performance of position control. In this study, Industrial Emulator is used. The inertia of it can fluctuate by putting some weights on Drive Disc and Load Disc. A controller which guarantees robust stability to variation of the inertia. By using H_∞ control, the disturbance is guaranteed. The effectiveness of proposed method is verified by simulation results.

1 Introduction

A machine which convey rotary power with belt and gear are used to timing belt of a car engine, machine tool, belt conveyor, and so on. In the spot of a manufacturing, it is indispensable. A lot of studies of the machine which convey rotary power with belt and gear are considered [2] [3] [4] [5]. There is a gap between gear and gears or gear and belts. The gap expresses backlash. However, the backlash has a big problem. When rotation of the gear turned over, the gear cannot introduce the rotary power into the size of the backlash. The backlash cause a position gap and limit cycle. Therefore, considering backlash is necessary to realize accurate performance of position control [2] [3] [4]. In the real spot, a parameter variation by abrasion of a part and disturbance is considered. It is necessary to guarantee the robust stability [5]. The object of this study is to improve a performance of positioning control for Industrial Emulator. The modeling including backlash is derived. And the backlash is modeled by using Dead-zone Model [2] [3]. Furthermore, the controller in consideration of backlash and parameter variation caused by variation of inertia moment is designed. Here, for the backlash, H_∞ controller is designed. And, for the parameter variation, robust controller is designed. Finally, the effectiveness of proposed method is verified by simulation results.

2 modeling

2.1 Physical Parameter

The structure of control target is shown in Fig.1^[1]. Physical parameters used in this modeling is shown in Table1.

2.2 Motion Equation

Fig.2 shows a magnified figure of Drive Disc.

Where, $F_1(t)$, $F_2(t)$ is the tensions of the belt between Drive Disc and Idler Pulleys. c_d is viscosity friction coefficient of Drive Disc. Motion equation of Drive Disc is shown as follows.

$$J_d \ddot{\theta}_d(t) = \tau(t) - c_d \dot{\theta}_d(t) + \{F_1(t) - F_2(t)\} r_d \quad (1)$$

Fig.3 shows a magnified figure of Load Disc.

Table 1 Physical Parameters

Drive Disc angle	θ_d	[rad]
Load Disc angle	θ_l	[rad]
Idler Pulleys angle	θ_p	[rad]
Radius of Drive Disc	r_d	[m]
Radius of Load disc	r_l	[m]
Radius of Bottom Pulley	r_{pd}	[m]
Radius of Top Pulley	r_{pl}	[m]
Input torque to Drive Disc	τ	[Nm]
Moment of Drive Disc	J_d	[kgm ²]
Moment of Load Disc	J_l	[kgm ²]
Moment of Idler Pulleys	J_p	[kgm ²]
Viscosity friction coefficient of Drive Disc	c_d	[Nm/(rad/s)]
Viscosity friction coefficient of Load Disc	c_l	[Nm/(rad/s)]

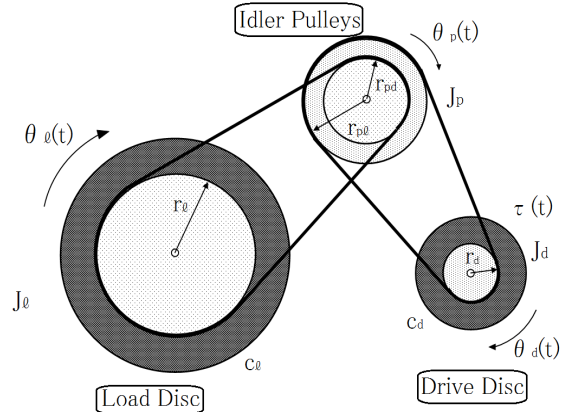


Fig. 1 Industrial Emulator

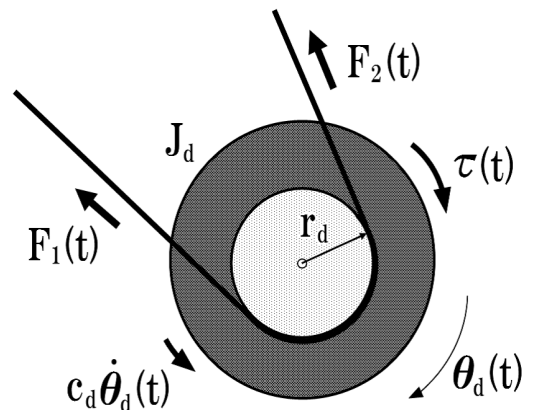


Fig. 2 Drive Disc

Where, $F_3(t)$, $F_4(t)$ is the tension in the belt between Idler Pulleys and Load Disc. c_l is viscosity friction coefficient of Load Disc. Motion equation of Load Disc is

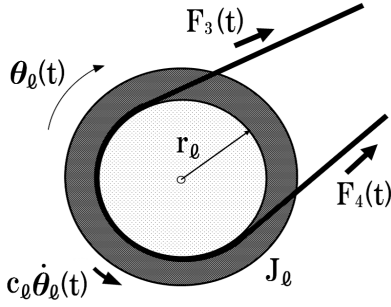


Fig. 3 Load disc

shown as follows.

$$J_l \ddot{\theta}_l(t) = -c_l \dot{\theta}_l(t) + \{F_3(t) - F_4(t)\} r_l \quad (2)$$

Fig.4 shows a magnified figure of Idler Pulleys.

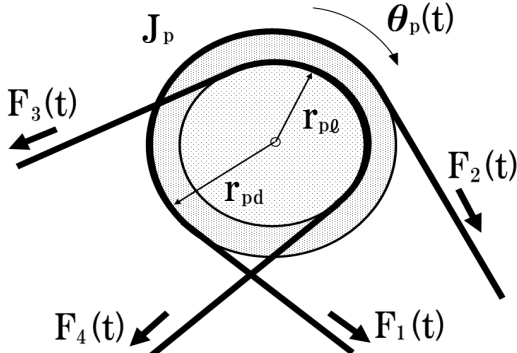


Fig. 4 Idler Pulleys

Motion equation of Idler Pulleys is shown as follows.

$$J_p \ddot{\theta}_p(t) = \{F_2(t) - F_1(t)\} r_{pd} + \{F_4(t) - F_3(t)\} r_{pl} \quad (3)$$

Here, the belt has elasticity in a property. Therefore, the belt regard as spring. The spring constant of the belt is defined as k_L . Then, let us regard the belts as a spring F_3 and F_4 are obtained as follows

$$F_3(t) = F_0 + k_L(r_{pl}\theta_p(t) - r_l\theta_l(t)) \quad (4)$$

$$F_4(t) = F_0 - k_L(r_{pl}\theta_p(t) - r_l\theta_l(t)) \quad (5)$$

Where, motion equation of Load Disc and Idler Pulleys are rewritten as follows.

$$J_l \ddot{\theta}_l(t) = -c_l \dot{\theta}_l(t) + 2k_L \{r_{pl}\theta_p(t) - r_l\theta_l(t)\} r_l \quad (6)$$

$$F_2(t) - F_1(t) = \frac{1}{r_{pd}} [J_p \ddot{\theta}_p(t) + 2k_L \{r_{pl}\theta_p(t) - r_l\theta_l(t)\} r_{pl}] \quad (7)$$

$$(8)$$

$$(9)$$

For the simplification of the equation, let K be as follows.

$$K := 2k_L r_l^2 \quad (10)$$

From Eq.(6), (9) and (10), motion equation are rewritten as follows.

$$J_d \ddot{\theta}_d(t) + \frac{r_d}{r_{pd}} J_p \ddot{\theta}_p(t) = \tau(t) - c_d \dot{\theta}_d(t) \quad (11)$$

$$-\frac{r_d}{r_{pd}} K \left\{ \frac{r_{pl}^2}{r_l^2} \theta_p(t) - \frac{r_{pl}}{r_l} \theta_l(t) \right\} \quad (12)$$

$$J_l \ddot{\theta}_l(t) = -c_l \dot{\theta}_l(t) + K \left\{ \frac{r_{pl}}{r_l} \theta_p(t) - \theta_l(t) \right\} \quad (13)$$

Here, the gear ratio between Drive Disc to Load Disc and between Drive Disc and Idler Pulleys are defined as follows.

$$g_r = \frac{r_l r_{pl}}{r_{pd} r_d} \quad (14)$$

$$g'_r = \frac{r_{pd}}{r_d} \quad (15)$$

From Eq.(14), (15), the following equation is expressed angle of the Drive Disc and Load Disc

$$\theta_d = g_r \theta_l \quad (16)$$

The following equation is expressed the Drive Disc and Idler Pulleys

$$\theta_d = g'_r \theta_p \quad (17)$$

From Eq.(14) (15), the following equation are obtained.

$$(J_d + g'_r J_p) \ddot{\theta}_d(t) = \tau(t) - c_d \dot{\theta}_d(t) - g_r^{-1} K \{g_r^{-1} \theta_d(t) - \theta_l(t)\} \quad (18)$$

$$J_l \ddot{\theta}_l(t) = -c_l \dot{\theta}_l(t) + K \{g_r^{-1} \theta_d(t) - \theta_l(t)\} \quad (19)$$

Where, the following expression is defined to simplify Eq.(20).

$$J_d^* \cong J_d + g_r'^{-2} J_p \quad (20)$$

From Eq.(20), Eq.(18) is rewritten as follows.

$$J_d^* \ddot{\theta}_d(t) = \tau - c_d \dot{\theta}_d(t) - K (g_r^{-2} \theta_d(t) - g_r^{-1} \theta_l(t)) \quad (21)$$

Based on Eq.(19), (21), let us regard the belt as transmission. Then, the transmission torque is defined as follows.

$$T(t) := K \{g_r^{-1} \theta_d(t) - \theta_l(t)\} \quad (22)$$

Eq.(19) (21) is rewritten as follows by using (22).

$$J_d^* \ddot{\theta}_d(t) = \tau - c_d \dot{\theta}_d(t) - g_r^{-1} T(t) \quad (23)$$

$$J_l \ddot{\theta}_l(t) = -c_l \dot{\theta}_l(t) + T(t) \quad (24)$$

2.3 Dead-zone Model

When rotation of the gear turns over, backlash delays transmission of torque. Therefore, in this study, I consider that $T(t)$ in Eq.(23), (24) is influenced by backlash.

Backlash nonlinearity is captured here using the Dead-zone model. Dead-zone model can be expressed as follows.

$$D_\alpha(t) = \begin{cases} g_r^{-1} \theta_d - \theta_l - \alpha & (g_r^{-1} \theta_d - \theta_l > \alpha) \\ 0 & (|g_r^{-1} \theta_d - \theta_l| < \alpha) \\ g_r^{-1} \theta_d - \theta_l + \alpha & (g_r^{-1} \theta_d - \theta_l < -\alpha) \end{cases} \quad (25)$$

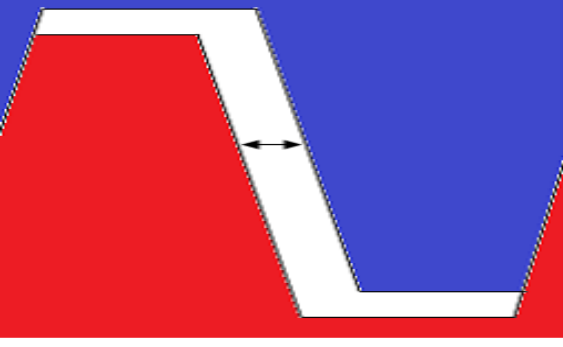


Fig. 5 Backlash

Where, α is backlash angle. $T(t)$ can be expressed as follows.

$$T(t) = KD_\alpha(\theta_d(t), \theta_l(t)) \quad (26)$$

And Eq.(25) is rewritten as follows.

$$D_\alpha(t) = g_r^{-1}\theta_d(t) - \theta_l(t) + d_\alpha(t) \quad (27)$$

Where, $d_\alpha(t)$ is defined as follows.

$$d_\alpha(t) = \begin{cases} -\alpha & (g_r^{-1}\theta_d - \theta_l > \alpha) \\ -g_r^{-1}\theta_d + \theta_l & (|g_r^{-1}\theta_d - \theta_l| < \alpha) \\ \alpha & (g_r^{-1}\theta_d - \theta_l < -\alpha) \end{cases} \quad (28)$$

By Eq.(25)–(28), motion equation of Drive Disc and Load Disc is given as follows.

$$J_d^* \ddot{\theta}_d(t) = \tau(t) - c_d \dot{\theta}_d(t) - K g_r^{-2} \theta_d(t) + K g_r^{-1} \theta_l(t) - K g_r^{-1} d_\alpha(t) \quad (29)$$

$$J_l \ddot{\theta}_l(t) = -c_l \dot{\theta}_l(t) + K g_r^{-1} \theta_d(t) - K \theta_l(t) + K d_\alpha(t) \quad (30)$$

2.4 State Space Representation

State variable, input and disturbance is defined as follows.

$$x(t) = [\theta_d, \theta_l, \dot{\theta}_d, \dot{\theta}_l]^T u(t) = \tau, w(t) = d_\alpha(t)$$

Then, the state space representation of industrial emulator is given as follows.

$$\begin{cases} \dot{x}(t) = Ax(t) + B_1 w(t) + B_2 u(t) \\ y(t) = Cx(t) \end{cases} \quad (31)$$

$$A = \begin{bmatrix} 0 & 1 & 0 & 0 \\ -\frac{K g_r^{-2}}{J_d^*} & -\frac{c_d}{J_d^*} & \frac{K g_r^{-1}}{J_d^*} & 0 \\ 0 & 0 & 0 & 1 \\ \frac{K g_r^{-1}}{J_l} & 0 & -\frac{K}{J_l} & -\frac{c_l}{J_l} \end{bmatrix}$$

$$B_1 = \begin{bmatrix} 0 \\ -\frac{K g_r^{-1}}{J_d^*} \\ 0 \\ \frac{K}{J_l} \end{bmatrix}, B_2 = \begin{bmatrix} 0 \\ \frac{1}{J_d^*} \\ 0 \\ 0 \end{bmatrix}, C = [0 \ 0 \ 1 \ 0]$$

2.5 Servo System

I designed a controller which makes to follow the control target. In order to remove a steady-state error, a servo system is used. Let $e(t)$ be the error between the output $y(t)$ and the reference $r(t)$. The state variable of the servo system satisfy $x_e(t)^T = [x(t) \int e(t)]^T$. The servo system can be expressed as follows.

$$\begin{cases} \dot{x}_e(t) = A_e x_e(t) + B_{1e} w(t) + B_{2e} u(t) \\ y(t) = C_1 e x_e(t) \end{cases} \quad (32)$$

Where, matrices A_e, B_{1e}, B_{2e} and C_1 are given as follows.

$$A_e = \begin{bmatrix} A & 0 \\ -C & 0 \end{bmatrix}, B_{1e} = \begin{bmatrix} B_1 & 0 \\ 0 & 1 \end{bmatrix}, B_{2e} = \begin{bmatrix} B_2 \\ 0 \end{bmatrix}$$

$$C_{1e} = [0 \ 0 \ 1 \ 0 \ 0]$$

3 Control Design

In this section, I design a controller which guarantees robust stability to variation of the inertias J_d^*, J_l .

3.1 Polytopic Representation

The range of the variation parameter J_d^*, J_l are as shown in Eq.(33), (34).

$$J_d^* \in [J_{d,min}^*, J_{d,max}^*] = [1.1 * 10^{-5}, 6.9 * 10^{-5}] \quad (33)$$

$$J_l \in [J_{l,min}, J_{l,max}] = [8.3 * 10^{-3}, 2.8 * 10^{-2}] \quad (34)$$

Then, the combination of fluctuation is shown as follows.

$$\{J_{d,min}^*, J_{l,min}\}, \{J_{d,max}^*, J_{l,min}\}, \{J_{d,min}^*, J_{l,max}\}, \{J_{d,max}^*, J_{l,max}\} \quad (35)$$

By using polytopic representation, the endpoints of variation range of matrices A_{ei}, B_{1ei}, B_{2ei} are shown as follows.

$$A_{ei} \ (i = 1, 2, 3, 4), B_{1ei} \ (i = 1, 2, 3, 4), B_{2ei} \ (i = 1, 2, 3, 4)$$

If each endpoint is stabilized, it may be said that it is stabilized at the endpoint interval.

3.2 H_∞ Control

H_∞ controller is designed. For Eq.(31), the general plant is defined as follows.

$$\begin{cases} \dot{x}_e(t) = A_e x_e(t) + B_{1e} w(t) + B_{2e} u(t) \\ z(t) = C_2 x_e(t) + D_2 u(t) \end{cases} \quad (36)$$

$$C_2 = \begin{bmatrix} W_x & 0 \\ 0 & W_e \\ 0 & 0 \end{bmatrix}, D_2 = \begin{bmatrix} 0 \\ 0 \\ W_u \end{bmatrix}$$

Where, $z(t)$ is cost function. $W_x \succ 0, W_e \succ 0$ and $W_u \succ 0$ are weight matrices for the state variable, integral and input. For the generalized plant, let us consider to minimize H_∞ norm from disturbance $w(t)$ to the cost output $z(t)$. Where, H_∞ norm is defined as follows.

$$\|G_{z\omega}(s)\| = \sup \frac{\|z(t)\|_\infty}{\|\omega(t)\|_\infty} \quad (37)$$

If there exist $\|G_{z\omega}(s)\| < \gamma_\infty$, the system is stabilized.

3.3 LMI Condition

The problem is formulated as follows.

Lemma 1 :If there exist X and Y satisfying the following LMIs, the system is stabilized by $u(t) = Kx_e(t) = YX^{-1}x_e(t)$.

minimize γ
subject to $X \succ 0$

$$\begin{bmatrix} XA_{ei}^T + A_{ei}X + Y^T B_{2ei} + B_{2ei}Y & XC_2^T + Y^T D_2^T & B_{1ei} \\ C_2X + D_2Y & -\gamma_\infty I & 0 \\ B_{1ei}^T & 0 & -\gamma_\infty I \end{bmatrix} \prec 0$$

($i = 1, 2, 3, 4$)
(38)

4 Simulation

In this section, the simulation results are shown. Furthermore, the proposed method is compared with the robust LQ controller. In this study, the backlash angle is defined as $0.6[\text{deg}] := 0.0105[\text{rad}]$ by system identification. A reference of the Load Disc angle is assigned $\frac{\pi}{2}$ [rad]. Simulation results of the Load Disc angle considering variation of the moment of Drive Disc and Load Disc are shown in Fig.6-9. The red line shows the Load Disc angle controlled by the H_∞ controller. The blue solid line shows the Load Disc angle controlled by the robust LQ. The black dot line shows reference.

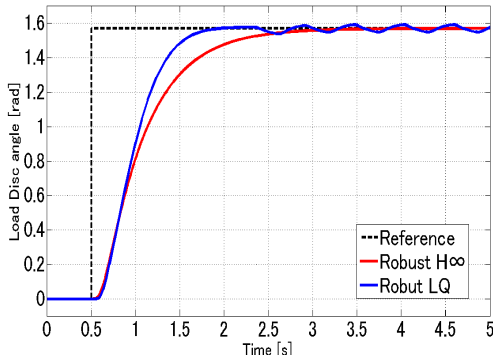


Fig. 6 J_{dmin}, J_{lmin}

As can be seen in Fig.6-9, the Load Disc angle stably follows the reference with the proposed method. However, the Load Disc angle does not follow the reference with the robust LQ. Even if there is the parameter variation, the Load Disc angle stably follows by H_∞ controller.

5 Conclusion

In this study, the modeling including backlash is derived by using Dead-zone model. H_∞ controller is designed for Industrial Emulator with backlash and parameter variation. The effectiveness of the proposed method is verified by simulation.

6 References

[1] Educational Control Products, 1995. Manual for Model 220 Industrial Emulator/Servo Trainer, California 91367, USA

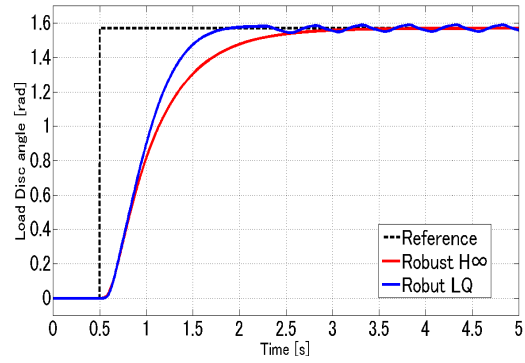


Fig. 7 J_{dmax}, J_{lmin}

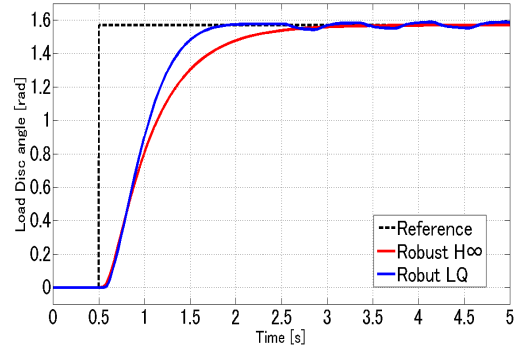


Fig. 8 J_{dmin}, J_{lmin}

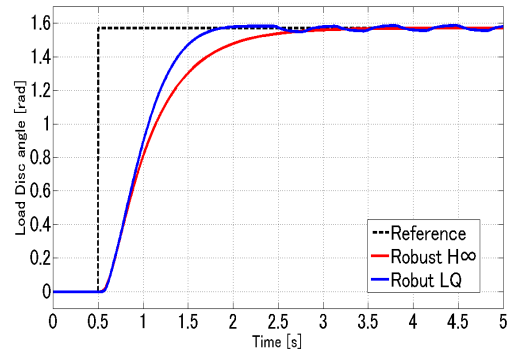


Fig. 9 J_{dmax}, J_{lmax}

[2] L.Acho, F.Ikhouane, and G.Pujol "Robust Control Design for Mechanisms with Backlash" JCET Vol.3 Iss.4 October 2013 PP. 175-180

[3] M. Nordin, P.O. Gutman, "Controlling mechanical systems with backlash: A survey", Automatica, Vol. 38, 2002, pp. 1633-1649.

[4] M. Nordin, J. Galic and P.O. Gutman, "New models for backlash and gear play", International Journal of Adaptive Control and Signal Processing, Vol. 11, No. 1, 1997, pp. 49-63. [doi: 10.1002/(SICI)1099-1115(199702)11:1]

[5] Orlov, Y., Aguilar, L.T., Alvarez, J., "Robust tracking control of servo systems with backlash: Nonsmooth H_∞ control vs. linear H_∞ control" American Control Conference (ACC), July 2015 pp.2051-2056